Article

Immunity

NAIP-NLRC4 Inflammasomes Coordinate Intestinal Epithelial Cell Expulsion with Eicosanoid and IL-18 Release via Activation of Caspase-1 and -8

Graphical Abstract

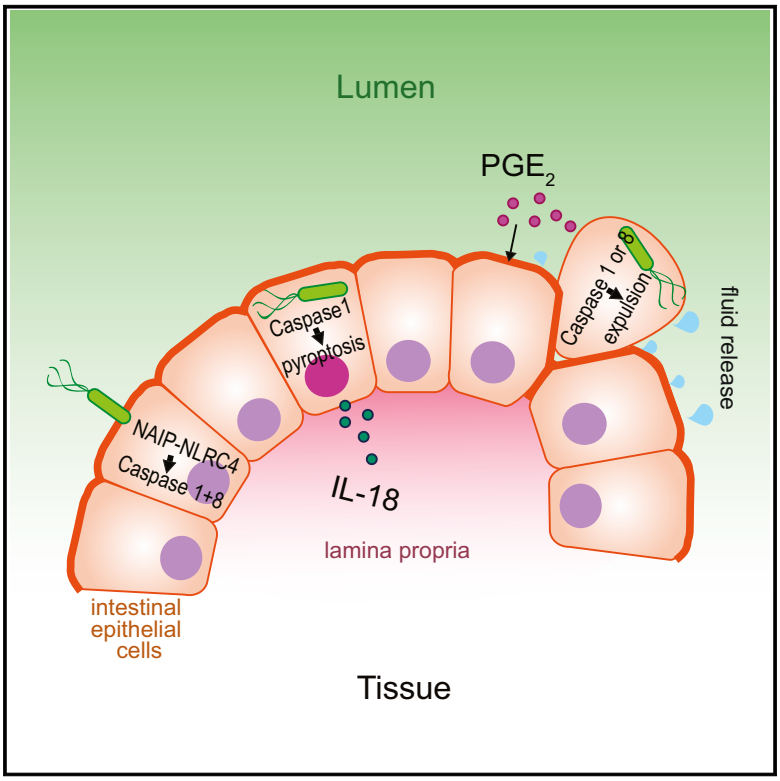

Authors

Isabella Rauch, Katherine A. Deets, Daisy X. Ji, ..., Igor E. Brodsky, Karsten Gronert, Russell E. Vance

Correspondence

rvance@berkeley.edu

In Brief

Rauch et al. show that selective activation of the NLRC4 inflammasome in intestinal epithelial cells leads to a coordinated response that includes cell expulsion and eicosanoid and cytokine release. This is not fully dependent on Caspase-1, as cell expulsion can also be caused by Caspase-8 activated by NLRC4.

Highlights

- NLRC4 activation in IECs leads to cell expulsion and IL-18 and eicosanoid release
- NLRC4 in IECs is sufficient to protect from infection but can cause pathology
- Caspase-1 and Gasdermin D are not necessary for NLRC4 signaling in IECs
- Caspase-8 is activated downstream of NLRC4

Rauch et al., 2017, Immunity *46*, 1–11
April 18, 2017
http://dx.doi.org/10.1016/j.immuni.2017.03.016

CellPress

Please cite this article in press as: Rauch et al., NAIP-NLRC4 Inflammasomes Coordinate Intestinal Epithelial Cell Expulsion with Eicosanoid and IL-18 Release via Activation of Caspase-1 and -8, Immunity (2017), http://dx.doi.org/10.1016/j.immuni.2017.03.016

CellPress

NAIP-NLRC4 Inflammasomes Coordinate Intestinal Epithelial Cell Expulsion with Eicosanoid and IL-18 Release via Activation of Caspase-1 and -8

Isabella Rauch,[1] Katherine A. Deets,[1] Daisy X. Ji,[1] Jakob von Moltke,[1,6] Jeannette L. Tenthorey,[1] Angus Y. Lee,[5] Naomi H. Philip,[2] Janelle S. Ayres,[1,7] Igor E. Brodsky,[2] Karsten Gronert,[3] and Russell E. Vance[1,4,5,8,*]
[1]Division of Immunology & Pathogenesis, Department of Molecular & Cell Biology, University of California, Berkeley, CA 94720, USA
[2]Department of Pathobiology, University of Pennsylvania School of Veterinary Medicine, Philadelphia, PA 19104, USA
[3]Vision Science Program, School of Optometry, University of California at Berkeley, Berkeley, CA 94720, USA
[4]Howard Hughes Medical Institute, University of California, Berkeley, CA 94720, USA
[5]Cancer Research Laboratory and Immunotherapeutics and Vaccine Research Initiative, University of California, Berkeley, CA 94720, USA
[6]Present address: Department of Immunology, University of Washington School of Medicine, Seattle, WA 98109, USA
[7]Present address: Nomis Center for Immunobiology and Microbial Pathogenesis, The Salk Institute for Biological Studies, La Jolla, CA 92037, USA
[8]Lead Contact
*Correspondence: rvance@berkeley.edu
http://dx.doi.org/10.1016/j.immuni.2017.03.016

SUMMARY

Intestinal epithelial cells (IECs) form a critical barrier against pathogen invasion. By generation of mice in which inflammasome expression is restricted to IECs, we describe a coordinated epithelium-intrinsic inflammasome response in vivo. This response was sufficient to protect against *Salmonella* tissue invasion and involved a previously reported IEC expulsion that was coordinated with lipid mediator and cytokine production and lytic IEC death. Excessive inflammasome activation in IECs was sufficient to result in diarrhea and pathology. Experiments with IEC organoids demonstrated that IEC expulsion did not require other cell types. IEC expulsion was accompanied by a major actin rearrangement in neighboring cells that maintained epithelium integrity but did not absolutely require Caspase-1 or Gasdermin D. Analysis of *Casp1*$^{-/-}$*Casp8*$^{-/-}$ mice revealed a functional Caspase-8 inflammasome in vivo. Thus, a coordinated IEC-intrinsic, Caspase-1 and -8 inflammasome response plays a key role in intestinal immune defense and pathology.

INTRODUCTION

Inflammasomes are cytosolic multi-protein complexes that initiate innate immune responses against invasive microbial pathogens by activating inflammatory caspases such as Caspase-1 (Lamkanfi and Dixit, 2014; Strowig et al., 2012). Although inflammasome components are broadly expressed, the role of inflammasomes has primarily been studied in hematopoietic cells. Studies of intestinal epithelial cells (IECs) suggest an epithelium-intrinsic role for the NLRP6 inflammasome in regulating inflammasome responses (Elinav et al., 2011; Levy et al., 2015; Sellin et al., 2015; Wlodarska et al., 2014), but whether NLRP6 itself forms an inflammasome or has other functions remains unclear (Anand et al., 2012). In addition, non-canonical human Caspase-4 and mouse Caspase-11 inflammasome activation has been implicated in epithelial responses upon infection (Knodler et al., 2014).

IECs also express NAIP-NLRC4 inflammasomes (Hu et al., 2010; Sellin et al., 2014). NAIP-NLRC4 inflammasomes are activated when bacterial protein ligands such as flagellin bind to NAIP family members, leading them to co-assemble with NLRC4 to form an inflammasome that activates Caspase-1 (Hu et al., 2015; Kofoed and Vance, 2011; Zhang et al., 2015; Zhao et al., 2011). Studies of human patients with gain-of-function *NLRC4* mutations suggest that NLRC4 activation can produce severe gut pathology, but whether this is due to hematopoietic or epithelial NLRC4 expression is unresolved (Canna et al., 2014; Romberg et al., 2014). In vivo studies of NLRC4-deficient animals demonstrated a role for NLRC4 in *Salmonella* infection (Broz et al., 2010; Carvalho et al., 2012; Franchi et al., 2012; Lara-Tejero et al., 2006; Mariathasan et al., 2004; Miao et al., 2010) and inflammation-induced colon cancer (Hu et al., 2010), but whether NLRC4 has an IEC-intrinsic function in these scenarios has not been addressed. Studies utilizing intestinal epithelium-specific NAIP-deficient mice demonstrated an epithelium-intrinsic requirement for NAIPs in *Salmonella* infection (Sellin et al., 2014) and colon tumorigenesis (Allam et al., 2015), but whether and/or how NLRC4 or Caspase-1 is involved remains unclear (Allam et al., 2015). A study using bone marrow transfer suggested that NLRC4 in non-hematopoetic cells is protective in infection with the epithelial cell-adhering pathogen *Citrobacter rodentium* (Nordlander et al., 2014), but interpretation of bone marrow chimeras is complicated by the possible presence of radioresistant hematopoietic cells. In macrophages, NAIP-NLRC4 activation results in Caspase-1-dependent processing and release of pro-inflammatory interleukins-1β and -18 and a lytic cell death called pyroptosis. By contrast, NAIP-NLRC4 activation in IECs was recently reported to result in their non-lytic expulsion into the gut lumen and protection from *Salmonella*

invasion (Sellin et al., 2014). Why macrophages but not epithelial cells would undergo pyroptosis upon Caspase-1 activation is not clear. In addition, whether inflammasome-dependent expulsion is an epithelial cell type-intrinsic response, or whether it involves other cell types, has not been addressed.

In this study, we provide genetic evidence for a coordinated intestinal epithelial cell-intrinsic inflammasome response in vivo. We demonstrate that IEC-specific activation of the NLRC4 inflammasome was sufficient to result in the production of eicosanoid lipid mediators, cell death accompanied by membrane permeability, and rapid IEC expulsion from the epithelial layer. The IEC inflammasome response did not absolutely require Caspase-1 or Gasdermin D, the known signaling components downstream of NLRC4 (Ding et al., 2016; Kayagaki et al., 2015). By generation of mice doubly deficient in Caspase-1 and Caspase-8, we have implicated Caspase-8 in NLRC4 inflammasome responses in vivo.

RESULTS

NLRC4 Induces Epithelium-Intrinsic Cell Expulsion, Fluid Loss, and Eicosanoid and IL-18 Release

To study cell type-specific roles of NLRC4, we engineered *Nlrc4*$^{-/-}$ mice to re-express NLRC4 from the *Rosa26* locus under Cre-inducible control (iNLRC4 mice; Figures 1A, S1A, and S1B). In these mice, Cre excises a floxed transcriptional STOP cassette that is upstream of *Nlrc4*. An internal ribosome entry site (IRES)-GFP reporter inserted downstream of *Nlrc4* allows identification of cells in which the STOP cassette has been excised. Crossing iNLRC4 mice to a *Vil1-cre* or *Lyz2-cre* transgene resulted in mice in which NLRC4 and GFP are expressed selectively in Villin^{+} IECs or LysM^{+} hematopoietic cells (monocytes, macrophages, granulocytes), respectively. To activate NLRC4 in the absence of potentially confounding Toll-like receptor (TLR) stimulation that accompanies bacterial infections, we used FlaTox, a previously described reagent for delivery of the NAIP5 ligand flagellin to the cytosol of cells (Ballard et al., 1996; Kofoed and Vance, 2011; von Moltke et al., 2012; Rauch et al., 2016; Zhao et al., 2011). As reported previously (von Moltke et al., 2012), systemic NAIP5-NLRC4 activation by FlaTox treatment of wild-type mice caused rapid hypothermia and vascular fluid loss, resulting in a marked increase in hematocrit, whereas *Nlrc4*$^{-/-}$ mice were fully protected from all symptoms (Figures 1B and 1C). Consistent with the previously described role of peritoneal macrophages in this phenotype (von Moltke et al., 2012), *Lyz2-cre*$^{+}$iNLRC4 mice succumbed to FlaTox with similar kinetics as wild-type mice. FlaTox-treated *Vil1-cre*$^{+}$ iNLRC4 mice that expressed NLRC4 only in IECs also experienced drastic hypothermia and a markedly increased hematocrit (Figures 1B and 1C). Furthermore, these mice also exhibited diarrhea, in contrast to mice expressing NLRC4 only in LysM^{+} myeloid cells (Figure 1D).

Eicosanoid lipid mediators, such as prostaglandins, can induce fluid loss and diarrhea and are a major contributor to the pathology caused by FlaTox (von Moltke et al., 2012). Therefore, we analyzed amounts of the prostaglandin PGE_2 in the intestinal tissue of our mice. Activation of NLRC4 only in IECs led to amounts of PGE_2 comparable to wild-type animals, demonstrating that inflammasome activation selectively in epithelial cells was sufficient to lead to local eicosanoid release (Figure 1E). Specific activation of NLRC4 in IECs was also sufficient to produce significant systemic amounts of interleukin-18 (Figure 1F), although NLRC4-mediated release of IL-18 by IECs was less than that released by myeloid cells (Figure S1C). Intestinal tissue-derived IL-18, however, seemed to be largely due to NLRC4 activation in epithelial cells (Figure S1C).

Most dramatically, histological analysis of small intestines from *Vil1-cre*$^{+}$iNLRC4 mice 60 min after FlaTox injection showed a massive expulsion of IECs into the intestinal lumen, causing marked villus blunting. Despite severe IEC sloughing, the intestinal epithelial layer appeared to remain contiguous over large areas, especially at early time points, though breakdown was evident by 60 min (Figure 1G). These results demonstrate that inflammasome activation selectively in epithelial cells is sufficient to result in a coordinated innate immune response involving eicosanoid and cytokine release, loss of fluid, and expulsion of IECs into the intestinal lumen.

Epithelial NLRC4 Is Sufficient to Protect against Intestinal *Salmonella* Invasion

To determine whether the epithelium-intrinsic inflammasome response was sufficient to protect against an invasive bacterial pathogen, we infected iNLRC4 mice with *Salmonella enterica* serovar Typhimurium (*S.* Typhimurium) and analyzed early tissue colonization. Expression of NLRC4 selectively in IECs was sufficient to significantly reduce bacterial colonization of cecum tissue compared to *Nlrc4*$^{-/-}$ mice (Figure 1H), whereas expression of NLRC4 selectively in myeloid cells had a minimal effect on cecum tissue colonization. Bacterial translocation to mesenteric lymph nodes, spleens, and livers trended lower in mice expressing NLRC4 in myeloid as well as in epithelial cells, though this decrease was not statistically significant (Figure S1D).

Inflammasome Activation Induces Cell-Autonomous Expulsion and Lytic Death of IECs

The above results demonstrated that NLRC4 activation selectively in intestinal epithelial cells was sufficient to induce pathology and protect against invasive bacterial pathogens, but did not address whether communication between epithelial cells and other cell types may also be involved in these responses. Therefore, to examine whether the NLRC4 inflammasome-induced cell expulsion of IECs is a cell type-autonomous process, we generated intestinal epithelial stem cell-derived organoids (Miyoshi and Stappenbeck, 2013) and treated these organoids with FlaTox. Intestinal organoids consist of pure cultures of epithelial cells, thereby eliminating contributions from other cell types. The organoid system provided the further advantage of allowing us to visualize inflammasome-dependent epithelial cell expulsion using live cell imaging (Figure 2A, upper row; Movie S1, left). Activation of NLRC4 in organoids led to dramatic cell expulsion and collapse of the organoid. Organoids derived from intestinal stem cells of *Nlrc4*$^{-/-}$ mice did not exhibit IEC expulsion upon FlaTox treatment (Movie S2). IEC expulsion was a remarkably rapid process, requiring ~6 min to complete, and was always unidirectional, with cells expelled selectively into the organoid lumen. Importantly, we observed that cells became permeable to

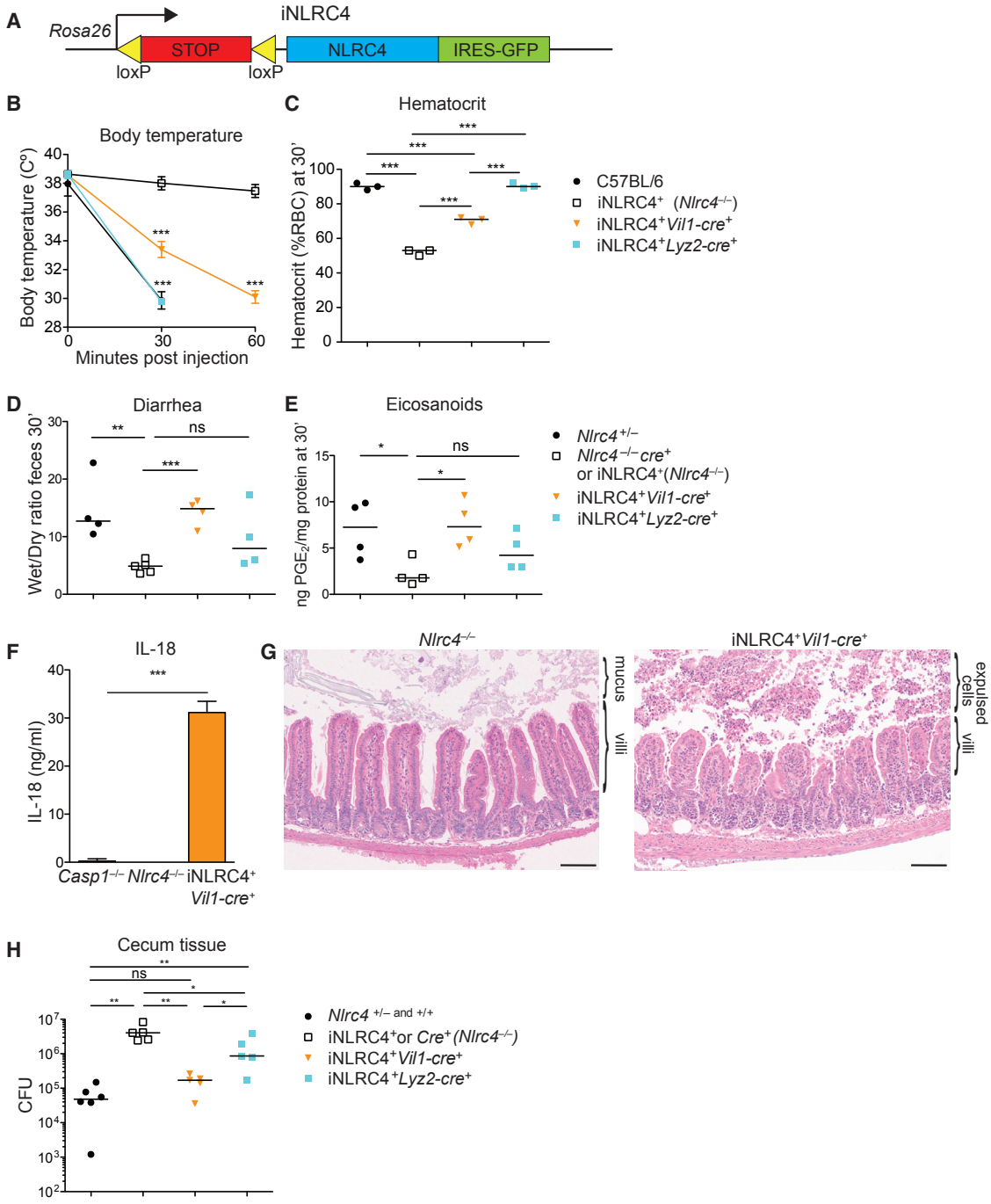

Figure 1. Specific Activation of NLRC4 in Intestinal Epithelial Cells Protects from Pathogen Invasion but Can Lead to Intestinal Pathology

(A) Schematic of the *Rosa26* locus after successful gene targeting with iNLRC4-IRES-GFP. Yellow triangles represent LoxP sites.

(B and C) Mice were injected with 0.8 μg/g PA and 0.4 μg/g LFn-Fla and monitored for (B) body temperature and (C) hematocrit (30 min, n = 3).

(D and E) Mice were injected with 0.8 μg/g PA and 80 ng/g LFn-Fla166 and (D) wet/dry ratio of intestinal content and (E) PGE_2 amounts of intestinal tissue from mice treated for 30 min were determined (n = 4–5).

(F) Quantification of serum IL-18 using ELISA in mice treated as in (B), 60 min time point (n = 3).

(G) H&E staining of small intestinal tissue from mice treated as in (B), 60 min after injection. Scale bars represent 100 μm.

(H) CFU in cecum 18 hr after oral *S*. Typhimurium infection (n = 5).

Data are representative of three independent experiments. Shown are (B, F) mean ± SD, (C–E, H) median, (B–E) unpaired t test (in B compared to *Nlrc4*$^{-/-}$), (H) Mann-Whitney test, *p < 0.01, **p < 0.005, ***p < 0.001. Please see also Figure S1.

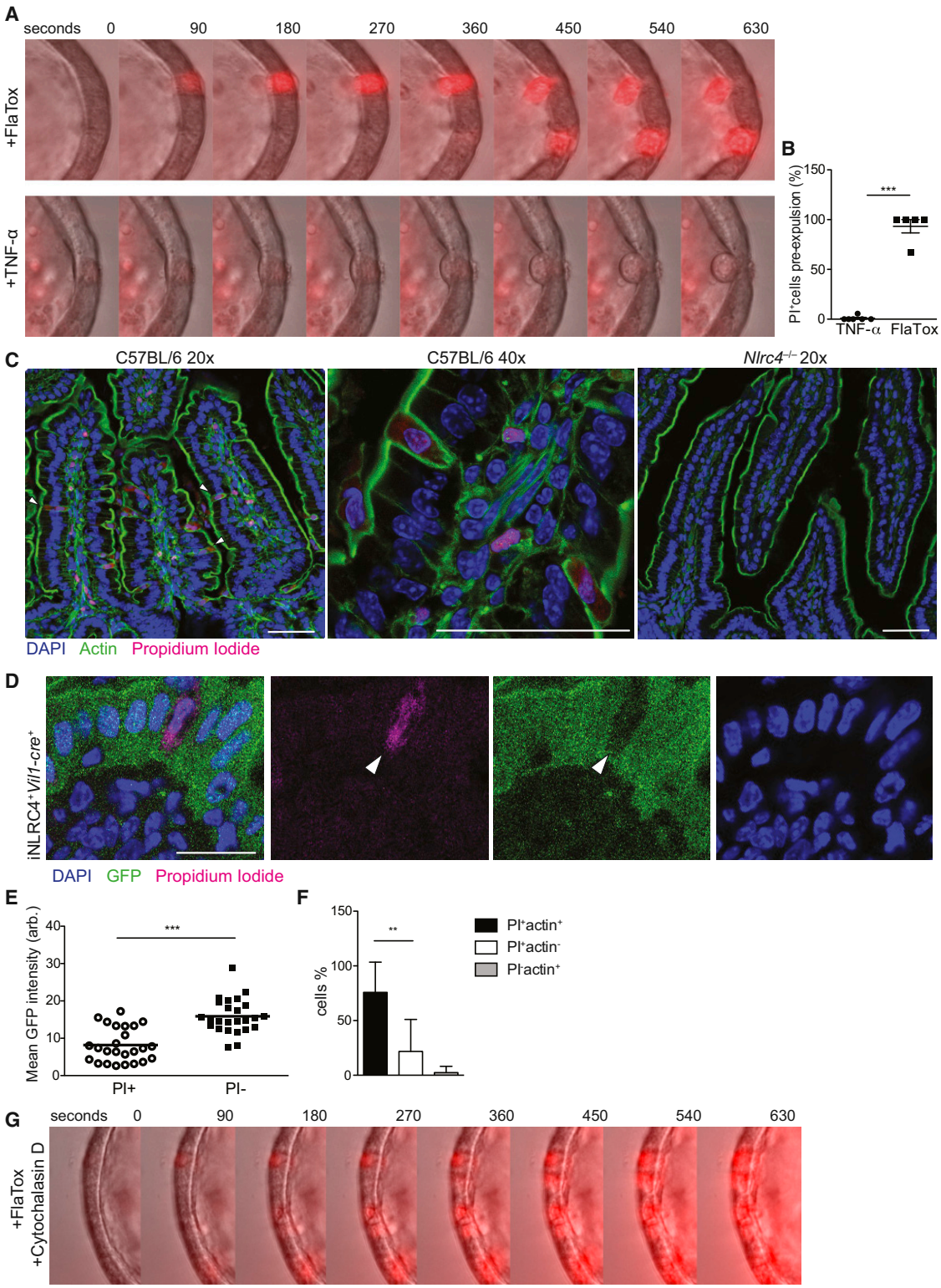

Figure 2. Cell-Autonomous Expulsion and Lytic Death of IECs

(A) Wild-type small intestinal organoid treated with 16 μg/mL of PA and 1 μg/mL LFn-Fla166 (top) or 100 ng/mL TNF-α (bottom) and stained with propidium iodide.

(B) Blinded quantification of C57BL/6 small intestinal organoid cells positive for propidium iodide before expulsion in Fla166Tox versus TNF-α treatment as in (A). n = 5–6 movies/ treatment; mean ± SEM.

(C and D) Propidium iodide and fluorescent phalloidin (actin) (C) or propidium iodide and GFP (D) in small intestines from mice treated with 0.2 μg/g of PA and 0.1 μg/g LFn-Fla for 60 min. Arrows indicate expulsing cells. Scale bars represent 40 (C) and 20 (D) μm.

(legend continued on next page)

propidium iodide (PI), a dye excluded from intact cells, prior to expulsion. The early loss of plasma membrane integrity is characteristic of pyroptotic cell death and distinguishes inflammasome-driven epithelial cell expulsion from previously reported mechanisms of epithelial cell expulsion (Eisenhoffer et al., 2012; Rosenblatt et al., 2001). Indeed, organoids treated with tumor necrosis factor-α (TNF-α) to induce apoptosis resulted in expulsion of intact (PI-negative) cells (Figures 2A, lower row, and 2B; Movie S1, right).

Our data suggest that inflammasome activation in IECs results in a loss of plasma membrane integrity and cell death that closely resembles pyroptotic cell death observed in macrophages (LaRock and Cookson, 2013). Our results differ from a previous report that concluded inflammasome activation in IECs does not result in pyroptosis (Sellin et al., 2014). However, this prior report assayed for plasma membrane integrity by observing whether tandem RFP protein is retained cytosolically in IECs. It is now appreciated that tandem RFP (60 kDa) (Campbell et al., 2002) is probably too large to escape rapidly through the ~10–16 nm Gasdermin D plasma membrane pores that form during pyroptosis (Aglietti et al., 2016; Ding et al., 2016). Also, in a *S*. Typhimurium-infected epithelial cell line, Caspase-1 activation and uptake of a cell viability dye have been reported prior to cell extrusion (Knodler et al., 2010). Thus, to assess whether IECs undergo pyroptosis-like death prior to expulsion in vivo, we injected FlaTox-treated mice with PI and performed histological analysis of small intestinal tissue (Figure 2C). Wild-type mice showed numerous PI^+ cells in the epithelial layer, indicating that they have lost plasma membrane integrity prior to expulsion. As a negative control, we failed to find any PI^+ IECs in *Nlrc4*$^{-/-}$ animals injected with FlaTox. We also examined colon tissue and colon-derived organoids and obtained similar results (Figures S2A and S2B). As further confirmation that inflammasome activation causes IECs to lose membrane integrity prior to expulsion, we examined leakage of GFP (26.9 kDa), which is co-expressed in IECs in our genetically targeted iNLRC4 mice and is small enough to escape through Gasdermin D pores. We found that PI^+ cells showed significantly lower GFP intensity than their PI-negative neighbors, suggesting a loss of cytoplasmic GFP after inflammasome activation (Figures 2D and 2E). Together these results show that NLRC4 inflammasome activation in intestinal epithelial cells leads to a lytic cell death, resembling pyroptosis, that is coordinated with IEC expulsion from the epithelial layer.

The apparent lysis of IECs while still within the intestinal epithelium might be expected to result in loss of the integrity of the epithelial layer, thereby compromising its important barrier function. However, we observed that a majority of IECs adjacent to the PI^+ epithelial cells formed an actin "purse-string" that appeared to effectively seal off the pyroptotic cell and ensure the continuity of the epithelial layer (Figures 2C and 2F). Formation of a similar actin structure has been observed previously in extrusion of pre-apoptotic cells from epithelia (Rosenblatt et al., 2001), but its function may be particularly important during inflammasome-dependent IEC expulsion, since this appears to be accompanied by death of epithelial cells while still in the epithelial layer.

To ascertain the role of actin during IEC expulsion, we added cytochalasin D, an inhibitor of actin polymerization, to FlaTox-treated organoids (Movie S3, left, and Figure 2G). Cells in cytochalasin D-treated organoids still became permeable to PI after FlaTox exposure, demonstrating that actin rearrangement is not required for pyroptosis of epithelial cells. However, these PI^+ (lysed) cells remained trapped in the epithelial monolayer and were not expelled. Similar results were obtained using jasplakinolide, an inhibitor of actin disassembly (Movie S3, right). Organoids treated with inhibitors only did not display any PI-positive cells; however, they did exhibit some disorganization at later time points, probably because regular actin modifications are important for monolayer stability (not shown). Taken together, these results support the idea that rapid actin rearrangement is important to prevent loss of barrier integrity upon epithelial cell pyroptosis.

Caspase-1 Is Required for IEC Pyroptosis but Not IEC Expulsion

In macrophages, Caspase-1 appears to be essential for NLRC4-induced pyroptosis and cytokine processing. In IECs, NLRC4-dependent IL-18 release also required Caspase-1 (Figures 1F and S1C; *Casp1* singly-deficient mice generated by CRISPR/Cas9; Figures S4A–S4C). However, Caspase-1 and -11-deficient mice nevertheless exhibited kinetically delayed hypothermia and hemoconcentration after injection with FlaTox (von Moltke et al., 2012). These effects were accompanied by significant epithelial cell expulsion (Figure 3A). The intestines of *Casp1*$^{-/-}$*Casp11*$^{-/-}$ mice injected with FlaTox and PI still showed the characteristic actin structures surrounding cells undergoing expulsion, but they did not exhibit any PI-positive cells (Figures 3A and 3B). Thus, NLRC4-dependent expulsion of IECs does not appear to require *Casp1*. To address the cell type-intrinsic function of *Casp1* in IECs, we generated inducible *Casp1* mice ("iCasp1 mice," analogous to iNLRC4 mice, see Figures S3A–S3D) and crossed these mice to the *Vil1-cre* and *Lyz2-cre* transgenic lines. Upon FlaTox treatment, *Vil1-cre*$^+$iCasp1 mice show a more severe loss of body temperature and increase in hematocrit, diarrhea, and tissue PGE_2 than *Casp1*$^{-/-}$*Casp11*$^{-/-}$ mice (Figures 3C and S3E–S3G), indicating that Caspase-1 expression in epithelial cells is sufficient to mediate rapid IEC pyroptotic cell death and intestinal pathology. Accordingly, we found PI^+ IECs in the intestines of *Vil1-cre*$^+$iCasp1 mice after FlaTox injection (Figures 3A and 3B). Similar to our observations in iNLRC4 mice, expression of Caspase-1 only in myeloid cells led to a phenotype similar to that seen in wild-type animals upon FlaTox injection (Figures 3C and S3E–S3G). Confirming our in vivo observations, when we treated intestinal organoids derived from *Casp1*$^{-/-}$ mice with FlaTox, we observed IEC expulsion, but importantly, the IECs did not become PI^+ prior to expulsion, in contrast to wild-type IECs (compare Figures 2A and 3D and Movies S1 and S4).

(E) Quantification of GFP signal in propidium iodide-positive and neighboring negative cells from samples as in (D) (n = 3; mean).
(F) Quantification of actin purse strings in propidium iodide-positive cells from samples as in (C) (n = 7; mean ± SD).
(G) Wild-type small intestinal organoid treated with 16 μg/mL of PA, 1 μg/mL LFn-Fla166, and 2.5 μM cytochalasin D and stained with propidium iodide.
Data representative of at least two independent experiments, unpaired t test, $^{**}p < 0.005$, $^{***}p < 0.001$. Please see also Figure S2.

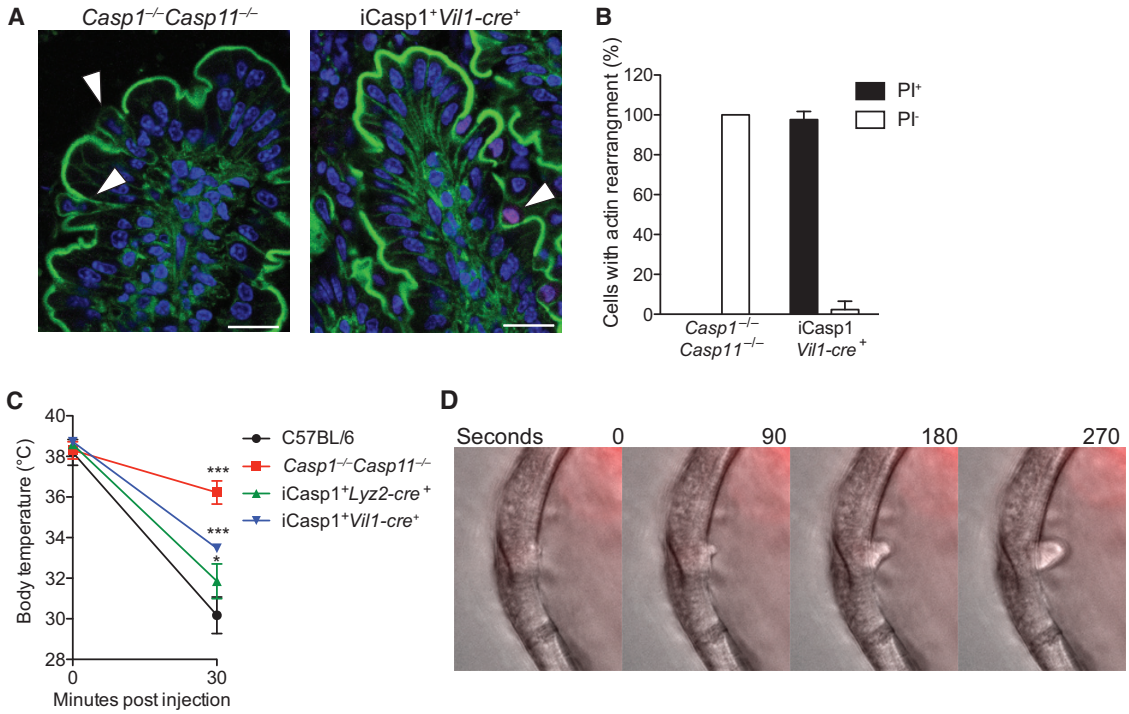

Figure 3. Caspase-1 Is Required for IEC Pyroptosis but Not IEC Expulsion

(A) Propidium iodide and fluorescent phalloidin (actin) in small intestines from mice treated with 0.8 μg/g PA and 0.4 μg/g LFn-Fla for 60 min. Arrows indicate expulsing cells. Scale bars represent 20 μm.

(B) Blinded quantification of propidium iodide-positive and -negative cells with actin purse strings in samples as in (A) (n = 3).

(C) Mice were treated as in (A) and monitored for body temperature (n = 3).

(D) *Casp1*$^{-/-}$ small intestinal organoid treated with 16 μg/mL of PA and 1 μg/mL LFn-Fla166 and stained with propidium iodide.

Data representative of at least two independent experiments. Shown are (B, C) mean ± SD, (C) unpaired t test compared to *Casp1*$^{-/-}$*Casp11*$^{-/-}$, ***p < 0.001. Please see also Figure S3.

Gasdermin D Is Required for IEC Pyroptosis but Not IEC Expulsion

Gasdermin D was recently identified as the main effector of pyroptosis downstream of Caspase-1 and -11 (Kayagaki et al., 2015; Shi et al., 2015). To determine whether *Gsdmd* is required for IEC pyroptosis-like death, we generated *Gsdmd*$^{-/-}$ mice using CRISPR/Cas9 (Figures S4D–S4F). We observed that FlaTox did not induce epithelial cell pyroptosis in *Gsdmd*$^{-/-}$ mice (Figures 4A and 4B). However, *Gsdmd*$^{-/-}$ mice were still susceptible to FlaTox and exhibited robust epithelial cell expulsion, indicating that the *Casp1*-independent effects of NLRC4 inflammasome activation in epithelial cells do not require Gasdermin D (Figures 4A, 4C, 4D, S4G, and S4H). Therefore, IEC pyroptotic-like death requires *Casp1* and *Gsdmd*, but even in the absence of *Casp1* and *Gsdmd*, a delayed non-pyroptotic NLRC4-dependent IEC expulsion and intestinal pathology can still occur.

ASC Is Required for Caspase-1-Independent NLRC4 Signaling

Casp1$^{-/-}$*Casp11*$^{-/-}$ mice additionally deficient for the inflammasome adaptor ASC (encoded by the *Pycard* gene) were completely protected from hypothermia upon systemic NLRC4 activation (Figure 5A). Phenocopying *Nlrc4*$^{-/-}$ mice, *Casp1*$^{-/-}$ *Casp11*$^{-/-}$ *Pycard*$^{-/-}$ mice were also protected from the FlaTox-induced increase in hematocrit and PGE_2 as well as diarrhea (Figures 5B and S3E–S3G) and epithelial cell expulsion (Figure 5C). Loss of ASC alone did not confer any significant protection. Taken together, the above results suggest that NLRC4 activation in IECs can result in *Casp1*-dependent *Pycard*-independent pyroptosis, as well as a *Pycard*-dependent response that does not require *Casp1* and is sufficient to induce IEC expulsion and intestinal pathology.

A Caspase-8 Inflammasome Compensates for Loss of Caspase-1

We sought to determine how NLRC4 induces IEC expulsion and intestinal pathology independent of *Casp1* and *Gsdmd*. Caspase-8 can bind the Pyrin domain of ASC (Masumoto et al., 2003) and has been reported to be recruited to the NLRC4 inflammasome ASC speck upon *Salmonella* infection of macrophages (Man et al., 2013). However, loss of *Casp8* did not affect cell death in this context, possibly because of compensation from *Casp1*. Caspase-8 has also been reported to function in NLRP3-induced IL-1β release (Antonopoulos et al., 2015; Karki et al., 2015). However, these experiments did not exclude the possibility that Caspase-8 is required for transcriptional priming upstream of NLRP3 or pro-IL-1β, rather than for signaling downstream of inflammasome activation (Antonopoulos et al., 2015; Gurung and Kanneganti, 2015; Karki et al., 2015; Man et al., 2013). In contrast to NLRP3, the NLRC4 inflammasome does not require

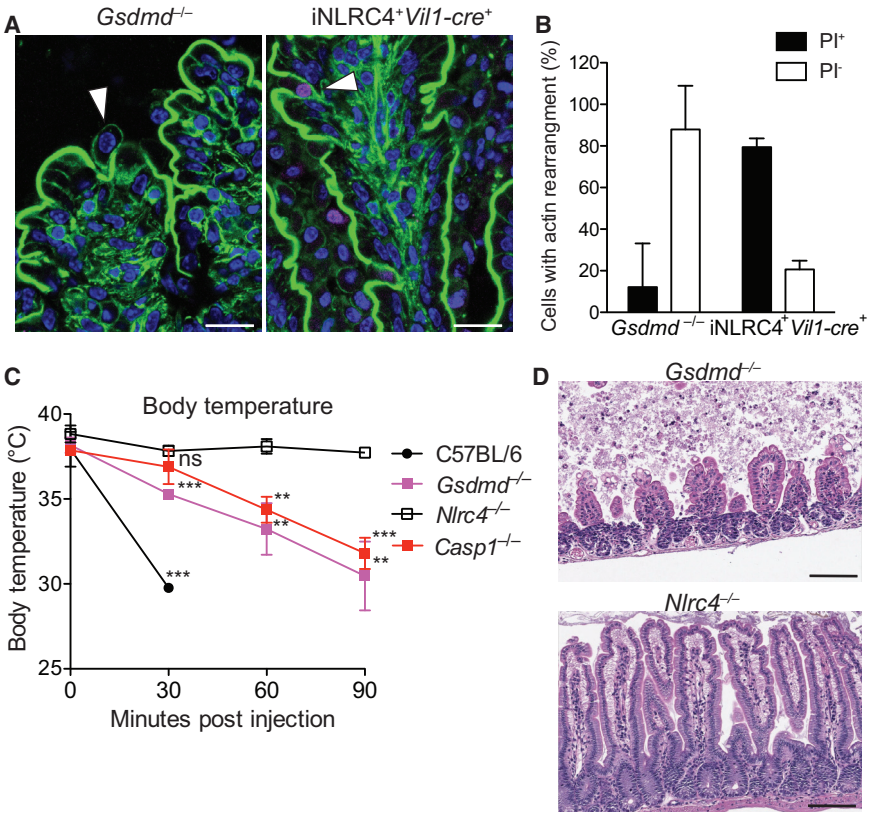

Figure 4. Gasdermin D Is Required for IEC Pyroptosis but Not IEC Expulsion

(A) Propidium iodide and fluorescent phalloidin (actin) in small intestines from mice treated with 0.8 μg/g PA and 0.4 μg/g LFn-Fla for 60 min. Arrows indicate expulsing cells. Scale bars represent 20 μm.

(B) Blinded quantification of propidium iodide-positive and -negative cells with actin purse strings in samples as in (A) (n = 3).

(C) Mice were injected with 0.8 μg/g PA and 0.4 μg/g LFn-Fla and monitored for body temperature (n = 3).

(D) H&E staining of small intestinal tissue from mice treated as in (A), 90 min time point. Scale bars represent 100 μm.

Data representative of at least two independent experiments. Shown are (B, C) mean ± SD, (C) unpaired t test compared to *Nlrc4*$^{-/-}$,**p < 0.005, ***p < 0.001. Please see also Figure S4.

transcriptional priming, and epithelial cell expulsion is a rapid, transcription-independent process. Thus, we sought to take advantage of our experimental system to establish a functional role for Caspase-8 downstream of NLRC4 inflammasome activation in vivo. Since loss of *Casp8* results in *Ripk3*-dependent embryonic lethality, we used CRISPR/Cas9 to create *Casp8*-deficient mice on a *Casp1*$^{-/-}$*Ripk3*$^{-/-}$ background (Figures S5A and S5B). Remarkably, the *Casp1*$^{-/-}$*Casp8*$^{-/-}$*Ripk3*$^{-/-}$ mice were fully protected from FlaTox and phenocopied the complete resistance of *Nlrc4*$^{-/-}$ mice to inflammasome-induced hypothermia, hematocrit increase, diarrhea, and IEC expulsion (Figures 6A, 6B, S5C, and S5D). By contrast, *Casp8*$^{-/-}$*Ripk3*$^{-/-}$, *Casp1*$^{-/-}$*Ripk3*$^{-/-}$, and *Ripk3*$^{-/-}$ mice exhibited robust FlaTox-induced pathology (Figures 6A and 6B). Furthermore, *Casp8*$^{-/-}$*Ripk3*$^{-/-}$ organoids treated with Flatox showed expulsion of PI-permeable cells (Movie S5), demonstrating that although Caspase-1 is not essential to mediate the effects of NLRC4 activation in IECs, it is sufficient. Accordingly, organoids derived from *Casp1*$^{-/-}$*Casp8*$^{-/-}$*Ripk3*$^{-/-}$ mice were completely protected from NLRC4-induced epithelial cell expulsion (Movie S6). PGE_2 amounts in intestines of *Ripk3*$^{-/-}$*Casp8*$^{-/-}$ mice injected with FlaTox were not decreased compared to controls (Figure 6C). There was, however, an apparent (but not statistically significant) decrease of PGE_2 in *Ripk3*$^{-/-}$*Casp1*$^{-/-}$ intestines and a further statistically significant decrease in *Casp1*$^{-/-}$*Casp8*$^{-/-}$*Ripk3*$^{-/-}$ tissue as compared to *Ripk3*$^{-/-}$ controls (Figure 6C). Thus, both Casp1 and Casp8 contribute to the coordinated production of eicosanoids that accompany IEC expulsion downstream of NLRC4 activation. To further address cell type specificity of this response, we treated organoids with FlaTox in vitro and analyzed supernatants for PGE_2 (Figure S5E). All organoids except *Nlrc4*$^{-/-}$ and *Casp1*$^{-/-}$*Casp8*$^{-/-}$*Ripk3*$^{-/-}$ organoids released significant amounts of PGE_2 over background, confirming that the eicosanoid pathway is cell autonomously active in IECs.

As an additional approach to establish cell type-specific roles of Caspase-1 and -8, we generated bone marrow chimeras in which *Casp1*$^{-/-}$*Casp8*$^{-/-}$*Ripk3*$^{-/-}$ bone marrow was used to reconstitute *Casp1*$^{-/-}$*Casp11*$^{-/-}$ hosts. In these chimeras, the only functional NLRC4-activated caspase is Caspase-8 in stromal cells, including IECs. The chimeras showed a robust hypothermic, hematocrit, and diarrhea response to FlaTox, only marginally less than the response of control chimeras in which *Casp1*$^{-/-}$*Casp11*$^{-/-}$ mice were reconstituted *Ripk3*$^{-/-}$*Casp1*$^{-/-}$ bone marrow (in which Casp8 is present in both hematopoietic and non-hematopoietic cells). These results suggest that Caspase-8 functions in radioresistant cells in vivo (Figures S5F–S5H).

Because radiation chimeras contain numerous radioresistant cells, potentially including radioresistant hematopoietic cells, the above bone marrow chimera experiment does not demonstrate that Caspase-8 functions in IECs. To address whether Caspase-8 is activated in IECs in vivo, we performed immunohistochemistry to detect cleaved Caspase-8. Intestines of FlaTox-injected wild-type and *Casp1*$^{-/-}$ mice showed cleaved Caspase-8 "specks," which were absent from intestines of FlaTox-treated *Nlrc4*$^{-/-}$, *Casp8*$^{-/-}$*Ripk3*$^{-/-}$, or *Pycard*$^{-/-}$ animals (Figures S6A and S6B). Furthermore, using a reconstituted inflammasome system with epitope-tagged proteins expressed in 293T cells, we found that Caspase-8 co-immunoprecipitated with flagellin, NLRC4 and NAIP5 only in the presence of ASC (Figure S6C). Thus, taken together, our genetic, cell biological, and biochemical data strongly demonstrate that a functional NLRC4-Casp8 inflammasome is operational in IECs in vivo.

Finally, to ascertain a function for the NLRC4-Casp8 inflammasome in host defense, we infected *Casp1*$^{-/-}$*Ripk3*$^{-/-}$ mice with *S.* Typhimurium. Although these mice were susceptible

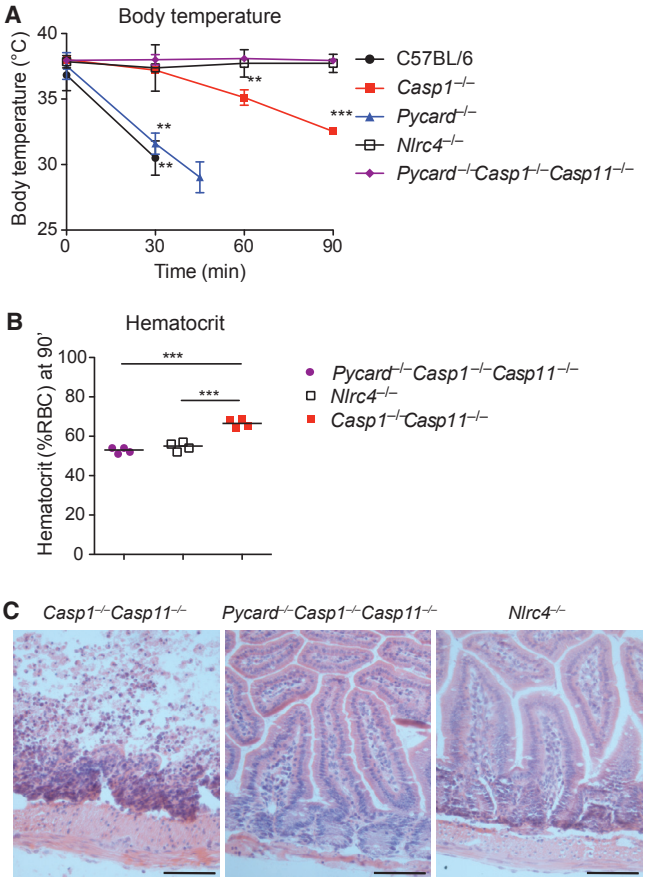

Figure 5. ASC Is Required for the Caspase1-Independent NLRC4 Signaling

(A and B) Mice were injected with 0.8 μg/g PA and 0.4 μg/g LFn-Fla and monitored for (A) body temperature and (B) hematocrit (90 min, n = 3).

(C) H&E staining of small intestinal tissue from mice treated as in (A), 90 min time point. Scale bars represent 100 μm.

Data representative of two independent experiments. Shown are (A) mean ± SD, (B) median. Unpaired t test (in A compared to *Nlrc4*$^{-/-}$), **p < 0.005, ***p < 0.001. Please see also Figure S3.

compared to wild-type or *Ripk3*$^{-/-}$ mice, they showed significantly lower tissue colonization than *Nlrc4*$^{-/-}$ animals (Figure 6D). This protection was lost upon additional deficiency of *Casp8*, as *Casp1*$^{-/-}$*Casp8*$^{-/-}$*Ripk3*$^{-/-}$ mice showed comparable tissue bacterial loads to *Nlrc4*$^{-/-}$ mice. These results demonstrate that in intestinal infections, Caspase-1 and -8 are activated downstream of NLRC4 to protect from pathogen invasion.

DISCUSSION

By generating mice in which expression of inflammasome components is restricted to intestinal epithelial cells, our results identify a unique and coordinated cell type-intrinsic response of IECs upon NLRC4-Caspase-1 and/or Caspase-8 inflammasome activation in vivo. We have shown the NLRC4-induced response involves a *Casp1*- and *Gsdmd*-dependent pyroptosis-like loss of epithelial cell plasma membrane integrity. This cell death was coordinated with a rapid expulsion of the pyroptotic IEC from the epithelial layer, a process that we showed was epithelial cell intrinsic. IEC expulsion appears to play an important role in limiting bacterial penetration into deeper tissues (Figure 1H; Sellin et al., 2014). We also showed that IEC expulsion was coordinated with epithelial cell production of IL-18 as well as of eicosanoid lipid mediators such as PGE_2 that trigger vascular leakage and fluid accumulation in the intestinal lumen. We propose that the eicosanoid-induced fluid response acts in concert with IEC expulsion, providing a mechanism in which expelled infected cells can be flushed from the intestines. The released IL-18 is probably critical to recruit immune cells that prevent dissemination of bacteria that managed to traverse the epithelium at later time points (Müller et al., 2016). Importantly, at moderate, physiologically relevant amounts, controlled permeabilization and expulsion of epithelial cells does not appear to result in overt destruction of the epithelium. Instead, we found that neighboring epithelial cells rapidly rearranged their actin cytoskeleton to accommodate the loss of the expulsed cell. Importantly, we provide genetic evidence that a *Casp8*-dependent inflammasome response can also mediate IEC expulsion, eicosanoid release, and protection from pathogen invasion, even in the absence of *Casp1*. Unlike previous studies, our results are not likely confounded by the effects of Caspase-8 deficiency on transcription, as our use of FlaTox allows us to selectively activate NLRC4, and NLRC4 activation does not require transcriptional priming. We speculate that the alternative NLRC4- and Caspase-8-dependent pathway might be important to provide resistance to bacterial pathogens that inhibit Caspase-1. Thus, taken together, our results define how inflammasome activation leads to a multi-faceted and coordinated epithelial cell response—involving cell death, expulsion, eicosanoid release, and actin remodeling—that is sufficient to provide protection from an invasive bacterial pathogen such as *Salmonella*. However, we also demonstrate that if this coordinated response is activated excessively, it can lead to major epithelial destruction and systemic pathology. We propose that the coordinated NLRC4-dependent response of epithelial cells probably contributes to intestinal pathology in humans with NLRC4 gain-of-function mutations (Canna et al., 2014; Romberg et al., 2014) and possibly other inflammatory bowel diseases as well.

EXPERIMENTAL PROCEDURES

Mouse Experiments

All mice used were specific pathogen free, maintained under a 12-hr light-dark cycle (7 am to 7 pm), and given a standard chow diet (Harlan irradiated laboratory animal diet) ad libitum. Wild-type C57BL/6J mice were originally obtained from the Jackson Laboratories, *Nlrc4*$^{-/-}$ animals were from V. Dixit (Genentech) (Mariathasan et al., 2004), *Casp1*$^{-/-}$*Casp11*$^{-/-}$ mice were provided by A. Van der Velden and M. Starnbach (Li et al., 1995), and *Ripk3*$^{-/-}$ mice were originally from Xiaodong Wang (He et al., 2009) and backcrossed to C57BL/6 by Astar Winoto. CRISPR/Cas9 targeting was performed by pronuclear injection of Cas9 mRNA and sgRNA into fertilized zygotes from colony-born mice, essentially as described previously (Wang et al., 2013). *Casp8*$^{-/-}$*Ripk3*$^{-/-}$ *Casp1*$^{-/-}$ mice were generated by targeting *Casp8* using CRISPR-Cas9 in *Casp1*$^{-/-}$*Ripk3*$^{-/-}$ mice. Founder mice were genotyped as described below, and founders carrying mutations were bred one generation to C57BL/6J mice to separate modified haplotypes. Homozygous lines were generated by interbreeding heterozygotes carrying matched haplotypes. iNLRC4 and iCasp1 mice were generated by targeting the *Rosa26* locus for genomic insertion of a construct encoding a loxP-flanked transcriptional STOP cassette

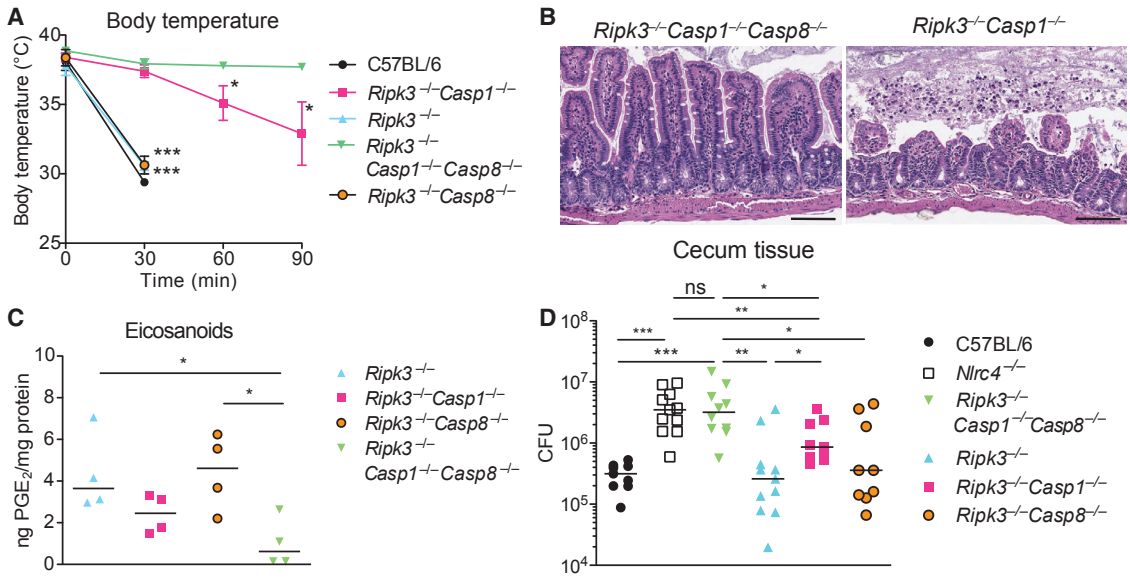

Figure 6. A Caspase-8 Inflammasome Compensates for Loss of Caspase-1

(A) Mice were injected with 0.8 μg/g PA and 0.4 μg/g LFn-Fla and monitored for body temperature (n = 3), mean ± SD.

(B) H&E staining of small intestinal tissue from mice treated as in (A), 90 min time point. Scale bars represent 100 μm.

(C) PGE_2 amounts of intestinal tissue from mice treated as in (A) for 30 min were determined (n = 4/group), median. Data representative of two independent experiments.

(D) CFU in cecum 18 hr after oral *S.* Typhimurium infection (n = 10), combined data of two independent experiments, median.

Shown are (A, C) unpaired t test (in A compared to *Ripk3*$^{-/-}$*Casp1*$^{-/-}$*Casp8*$^{-/-}$), (D) Mann-Whitney test, *p < 0.01, **p < 0.005, ***p < 0.001. Please see also Figures S5 and S6.

(Srinivas et al., 2001) upstream of the *Nlrc4* or *Casp1* cDNA transgene in JM8.F6 ES cells. An IRES-GFP (Sasaki et al., 2006) was included downstream of the *Nlrc4* or *Casp1* cDNA to mark cells in which the STOP cassette has been excised. Founders were crossed to the respective gene-deficient background (i.e., *Nlrc4*$^{-/-}$ or *Casp1*$^{-/-}$*Casp11*$^{-/-}$) and then further to *Vil1-cre* (Jax strain 004586) or *Lyz2-cre* (Jax strain 004781) transgenic lines. For bone marrow chimeras, mice were irradiated first with 500 and then 400 rad 4 hr apart and reconstituted with 5 × 10^6 donor cells by retrorbital injection. Chimeric mice were assayed 7 weeks after irradiation.

Animals used in infection and FlaTox injection experiments were littermates or, if not possible, cohoused upon weaning. All animal experiments complied with the regulatory standards of, and were approved by, the University of California Berkeley Institutional Animal Care and Use Committee.

Toxins

Recombinant proteins (PA, LFn-flagellin [*L. pneumophila* flagellin (FlaA; GenBank: YP_095369)], LFn-Fla166 [C-terminal 166 amino acids of FlaA]) were purified from insect cells. His_6-LFn fused to the N terminus of the indicated gene (Ser-Thr-Arg linker) or His_6-PA were cloned into pFastBacDual (Life Technologies) using the SalI and NotI restriction sites. Recombinant bacmids were generated to infect Sf9 cells according to the manufacturer's instruction. After 72 hr of infection with P2 baculovirus, insect cells were lysed with buffered detergent (1% NP-40 in 20 mM Tris, 150 mM NaCl [pH 8.0]) and then clarified by centrifugation at 50,000 × *g* for 45 min at 4°C. Proteins were purified using Ni-NTA agarose (QIAGEN), eluted with 500 mM imidazole in 20 mM Tris, 500 mM NaCl (pH 8.0), then dialyzed into 20 mM Tris (pH 8.0) and subjected to anion exchange chromatography (ENrich Q column, BioRad) using a gradient elution into high-salt buffer (20 mM Tris, 1 M NaCl [pH 8.0]). Fractions containing protein were concentrated using Amicon-Ultra centrifugal filters (EMD Millipore) and quantified using a BCA kit (Fisher Scientific). Endotoxin contamination of the preparations (determined using a LAL chromogenic endotoxin quantitation kit [Pierce]) was estimated to result in application of approximately 0.4 ng/mouse of endotoxin, an amount below the threshold for systemic responses in mice (Copeland et al., 2005).

Toxin doses were 0.2–0.8 μg/g body weight of PA combined with 0.1–0.4 μg/g LFn-Fla, or 20–80 ng/g LFnFla166 for intravenous (retro-orbital) delivery, or 16 μg/mL of PA combined with 1 μg/mL LFn-Fla166, for in vitro experiments. Rectal temperature was determined using a MicroTherma 2T thermometer (Braintree Scientific). Blood for hematocrit was collected by retroorbital bleed into StatSpin microhematocrit tubes (Fisher Scientific). For wet/dry ratio determination of intestinal contents, the content of the small intestine was placed into a tube, weighed, dried overnight in a 70°C incubator, and weighed again. For in vivo propidium iodide staining, mice were injected with 100 μg/mouse propidium iodide intravenously (retro-orbital) 10 min before sacrifice.

Salmonella Infections

Salmonella Typhimurium infections were performed as previously described (Barthel et al., 2003). In brief, 7- to 12-week-old mice deprived of food and water for 4 hr were gavaged with 25 mg streptomycin sulfate. 24 hr later, mice again deprived of food and water for 4 hr were gavaged with 3 × 10^7 CFUs *S.* Tm SL1344. Cecum tissue was incubated in PBS/400 mg/mL gentamycin for 30 min to kill extra-tissue bacteria and washed 6 times in PBS. Cecum and MLN were homogenized in sterile PBS and plated on MacConkey agar containing 50 mg/mL streptomycin.

Eicosanoid Analysis

To analyze PGE_2 tissue content using PGE2 EIA (Chayman chemicals), 100 mg of snap frozen jejunum were homogenized in 1 mL phosphate buffer (0.1 M phosphate [pH 7.4], containing 1 mM EDTA and 10 μM indomethacin) and prostaglandins were extracted as recommended by the manufacturer. In brief, proteins were precipitated with 4 mL ethanol followed by centrifugation at 3,000 × *g* for 10 min. Ethanol was evaporated under nitrogen and samples resuspended in ultrapure water and acidified to pH 4.0 with 1 M acetate buffer. Samples were applied to a methanol rinsed C-18 column, washed and eluted with 5 mL ethyl acetate containing 1% methanol. The ethyl acetate was

evaporated under a stream of nitrogen and samples resuspended in 500 μL EIA Buffer. EIA was performed according to manufacturer's instructions. PGE_2 amounts were normalized to protein content of the original sample, determined by BCA assay.

ELISA

Mice were bled retroorbitaly and serum analyzed by ELISA using paired IL- 18 Abs (BD Biosciences and eBioscience). For tissue cytokine amounts, snap frozen intestinal tissue was homogenized in PBS containing proteinase inhibitors (Pierce), spun at 18,000 × *g* and supernatants used for ELISA. Recombinant IL-18 (eBioscience) was used as a standard.

Histology and Histochemistry

For hematoxylin and eosin stainings, intact intestinal tissue was fixed for 24 hr in methacarn to preserve mucus and epithelial cells trapped inside the mucus. Tissue was paraffin embedded in a water-free procedure, cut to 5 μm, and stained. For analysis of cleaved Caspase 8, GFP, propidium iodide, and actin, intestinal tissue was sliced open and fixed in PLP buffer (0.05 M phosphate buffer containing 0.1 M L-lysine [pH 7.4], 2 mg/mL $NaIO_4$, and 1% PFA). After fixation overnight, tissue was washed in phosphate buffer and immersed in 30% sucrose overnight. Tissue was frozen in OCT, cut, and stained with 100 nM actistain 488 phalloidin (cytoskeleton) followed by DAPI. For cleaved Caspase 8 staining, slides were blocked using 10% normal donkey serum in 0.1% Tween20, 100 mM TrisHCl, 150 mM NaCl, 0.5% blocking reagent (Perkin Elmer) for 30 min. Slides were stained with 1:400 rabbit anti-mouse cleaved caspase-8 (no. 8592; Cell Signaling Technology) for 60 min followed by donkey anti rabbit Alexa Fluor 488 (JacksonImmunoReasearch) for 30 min, followed by DAPI.

Slides were analyzed on a Zeiss LSM710 and GFP intensity was measured using ImageJ software.

Organoids

Organoids from mouse small intestine were isolated and grown as previously described (Miyoshi and Stappenbeck, 2013). For live imaging, organoids were split into 8-well coverslides and 2 days after seeding preincubated with 100 μg/mL propidium iodide in growth medium for 30 min before treatment with Fla166Tox or TNFα in growth medium containing 100 μg/mL propidium iodide. For cytochalasin D treatment, organoids were incubated with FlaTox and 2.5 μM cytochalasin D was added 10 min later. For jasplakinolide treatment, 8 μM jasplakinolide was added at the same time as FlaTox. Live imaging was performed in an incubation chamber using a Nikon Widefield Epifluorescent Microscope. For eicosanoid measurements, organoids were differentiated as in Sato and Clevers (2013) with addition of 20 ng/mL IL-4 from day 3 on. On day 7, organoids were harvested in DPBS, seeded in 96- well plates, and treated with FlaTox. Supernatants were analyzed after 2 hr.

SUPPLEMENTAL INFORMATION

Supplemental Information includes six figures, six movies, and Supplemental Experimental Procedures and can be found with this article online at http://dx.doi.org/10.1016/j.immuni.2017.03.016.

AUTHOR CONTRIBUTIONS

I.R. and R.E.V. conceived the study, designed the experiments, and wrote the paper; I.R. performed the majority of the experiments; K.A.D. helped with organoid experiments and infections; A.Y.L. performed Cas9 mRNA/sgRNA injections into mouse zygotes; D.X.J. made *Gsdmd*$^{-/-}$ mice; J.L.T. performed co-immunoprecipitations; J.v.M. cloned the construct for the iCASP1 mice and generated the iNLRC4 mice to initiate the study; J.S.A. cloned the construct for the iNLRC4 mice; I.E.B. and N.H.P. helped with *Ripk3*$^{-/-}$*Casp8*$^{-/-}$ experiments; and K.G. provided reagents and expertise for eicosanoid analysis. All authors discussed the results and commented on the manuscript.

ACKNOWLEDGMENTS

We acknowledge the assistance of the UC Berkeley CRL Flow Cytometry Laboratory, Eric Chen, Peter Dietzen, Roberto Chavez, Jake Wu, and James Kang for technical support, the Vance and Barton Labs for discussions, and Greg Barton for comments on the manuscript. We thank Xiaodong Wang for *Ripk3*$^{-/-}$ mice and the Winoto Lab for backcrossing the mice to the C57BL/6 background. This work was supported by HHMI and NIH grants to R.E.V. (AI075039, AI063302) and NIH grant (EY026082) to K.G. R.E.V. was a Burroughs Wellcome Fund Investigator in the Pathogenesis of Infectious Disease and is an Investigator of the Howard Hughes Medical Institute. Research reported in this publication was supported in part by the NIH S10 program under award number 1S10RR026866-01. The content is solely the responsibility of the authors and does not necessarily represent the official views of the NIH. I.R. is supported by the Austrian Science Fund (FWF) (the Erwin Schrödinger Fellowship J3789-B22).

Received: August 26, 2016
Revised: December 9, 2016
Accepted: March 24, 2017
Published: April 11, 2017

REFERENCES

Aglietti, R.A., Estevez, A., Gupta, A., Ramirez, M.G., Liu, P.S., Kayagaki, N., Ciferri, C., Dixit, V.M., and Dueber, E.C. (2016). GsdmD p30 elicited by caspase-11 during pyroptosis forms pores in membranes. Proc. Natl. Acad. Sci. USA *113*, 7858–7863.

Allam, R., Maillard, M.H., Tardivel, A., Chennupati, V., Bega, H., Yu, C.W., Velin, D., Schneider, P., and Maslowski, K.M. (2015). Epithelial NAIPs protect against colonic tumorigenesis. J. Exp. Med. *212*, 369–383.

Anand, P.K., Malireddi, R.K.S., Lukens, J.R., Vogel, P., Bertin, J., Lamkanfi, M., and Kanneganti, T.-D. (2012). NLRP6 negatively regulates innate immunity and host defence against bacterial pathogens. Nature *488*, 389–393.

Antonopoulos, C., Russo, H.M., El Sanadi, C., Martin, B.N., Li, X., Kaiser, W.J., Mocarski, E.S., and Dubyak, G.R. (2015). Caspase-8 as an effector and regulator of NLRP3 inflammasome signaling. J. Biol. Chem. *290*, 20167–20184.

Ballard, J.D., Collier, R.J., and Starnbach, M.N. (1996). Anthrax toxin-mediated delivery of a cytotoxic T-cell epitope in vivo. Proc. Natl. Acad. Sci. USA *93*, 12531–12534.

Barthel, M., Hapfelmeier, S., Quintanilla-Martínez, L., Kremer, M., Rohde, M., Hogardt, M., Pfeffer, K., Rüssmann, H., and Hardt, W.-D. (2003). Pretreatment of mice with streptomycin provides a *Salmonella enterica* serovar Typhimurium colitis model that allows analysis of both pathogen and host. Infect. Immun. *71*, 2839–2858.

Broz, P., Newton, K., Lamkanfi, M., Mariathasan, S., Dixit, V.M., and Monack, D.M. (2010). Redundant roles for inflammasome receptors NLRP3 and NLRC4 in host defense against *Salmonella*. J. Exp. Med. *207*, 1745–1755.

Campbell, R.E., Tour, O., Palmer, A.E., Steinbach, P.A., Baird, G.S., Zacharias, D.A., and Tsien, R.Y. (2002). A monomeric red fluorescent protein. Proc. Natl. Acad. Sci. USA *99*, 7877–7882.

Canna, S.W., de Jesus, A.A., Gouni, S., Brooks, S.R., Marrero, B., Liu, Y., DiMattia, M.A., Zaal, K.J.M., Sanchez, G.A.M., Kim, H., et al. (2014). An activating NLRC4 inflammasome mutation causes autoinflammation with recurrent macrophage activation syndrome. Nat. Genet. *46*, 1140–1146.

Carvalho, F.A., Nalbantoglu, I., Aitken, J.D., Uchiyama, R., Su, Y., Doho, G.H., Vijay-Kumar, M., and Gewirtz, A.T. (2012). Cytosolic flagellin receptor NLRC4 protects mice against mucosal and systemic challenges. Mucosal Immunol. *5*, 288–298.

Copeland, S., Warren, H.S., Lowry, S.F., Calvano, S.E., and Remick, D.; Inflammation and the Host Response to Injury Investigators (2005). Acute inflammatory response to endotoxin in mice and humans. Clin. Diagn. Lab. Immunol. *12*, 60–67.

Ding, J., Wang, K., Liu, W., She, Y., Sun, Q., Shi, J., Sun, H., Wang, D.-C., and Shao, F. (2016). Pore-forming activity and structural autoinhibition of the gasdermin family. Nature *535*, 111–116.

Eisenhoffer, G.T., Loftus, P.D., Yoshigi, M., Otsuna, H., Chien, C.-B., Morcos, P.A., and Rosenblatt, J. (2012). Crowding induces live cell extrusion to maintain homeostatic cell numbers in epithelia. Nature *484*, 546–549.

Elinav, E., Strowig, T., Kau, A.L., Henao-Mejia, J., Thaiss, C.A., Booth, C.J., Peaper, D.R., Bertin, J., Eisenbarth, S.C., Gordon, J.I., and Flavell, R.A. (2011). NLRP6 inflammasome regulates colonic microbial ecology and risk for colitis. Cell *145*, 745–757.

Franchi, L., Kamada, N., Nakamura, Y., Burberry, A., Kuffa, P., Suzuki, S., Shaw, M.H., Kim, Y.-G., and Núñez, G. (2012). NLRC4-driven production of IL-1β discriminates between pathogenic and commensal bacteria and promotes host intestinal defense. Nat. Immunol. *13*, 449–456.

Gurung, P., and Kanneganti, T.-D. (2015). Novel roles for caspase-8 in IL-1β and inflammasome regulation. Am. J. Pathol. *185*, 17–25.

He, S., Wang, L., Miao, L., Wang, T., Du, F., Zhao, L., and Wang, X. (2009). Receptor interacting protein kinase-3 determines cellular necrotic response to TNF-alpha. Cell *137*, 1100–1111.

Hu, B., Elinav, E., Huber, S., Booth, C.J., Strowig, T., Jin, C., Eisenbarth, S.C., and Flavell, R.A. (2010). Inflammation-induced tumorigenesis in the colon is regulated by caspase-1 and NLRC4. Proc. Natl. Acad. Sci. USA *107*, 21635–21640.

Hu, Z., Zhou, Q., Zhang, C., Fan, S., Cheng, W., Zhao, Y., Shao, F., Wang, H.-W., Sui, S.-F., and Chai, J. (2015). Structural and biochemical basis for induced self-propagation of NLRC4. Science *350*, 399–404.

Karki, R., Man, S.M., Malireddi, R.K.S., Gurung, P., Vogel, P., Lamkanfi, M., and Kanneganti, T.-D. (2015). Concerted activation of the AIM2 and NLRP3 inflammasomes orchestrates host protection against *Aspergillus* infection. Cell Host Microbe *17*, 357–368.

Kayagaki, N., Stowe, I.B., Lee, B.L., O'Rourke, K., Anderson, K., Warming, S., Cuellar, T., Haley, B., Roose-Girma, M., Phung, Q.T., et al. (2015). Caspase-11 cleaves gasdermin D for non-canonical inflammasome signalling. Nature *526*, 666–671.

Knodler, L.A., Vallance, B.A., Celli, J., Winfree, S., Hansen, B., Montero, M., and Steele-Mortimer, O. (2010). Dissemination of invasive *Salmonella* via bacterial-induced extrusion of mucosal epithelia. Proc. Natl. Acad. Sci. USA *107*, 17733–17738.

Knodler, L.A., Crowley, S.M., Sham, H.P., Yang, H., Wrande, M., Ma, C., Ernst, R.K., Steele-Mortimer, O., Celli, J., and Vallance, B.A. (2014). Noncanonical inflammasome activation of caspase-4/caspase-11 mediates epithelial defenses against enteric bacterial pathogens. Cell Host Microbe *16*, 249–256.

Kofoed, E.M., and Vance, R.E. (2011). Innate immune recognition of bacterial ligands by NAIPs determines inflammasome specificity. Nature *477*, 592–595.

Lamkanfi, M., and Dixit, V.M. (2014). Mechanisms and functions of inflammasomes. Cell *157*, 1013–1022.

Lara-Tejero, M., Sutterwala, F.S., Ogura, Y., Grant, E.P., Bertin, J., Coyle, A.J., Flavell, R.A., and Galán, J.E. (2006). Role of the caspase-1 inflammasome in *Salmonella* typhimurium pathogenesis. J. Exp. Med. *203*, 1407–1412.

LaRock, C.N., and Cookson, B.T. (2013). Burning down the house: cellular actions during pyroptosis. PLoS Pathog. *9*, e1003793.

Levy, M., Thaiss, C.A., Zeevi, D., Dohnalová, L., Zilberman-Schapira, G., Mahdi, J.A., David, E., Savidor, A., Korem, T., Herzig, Y., et al. (2015). Microbiota-modulated metabolites shape the intestinal microenvironment by regulating NLRP6 inflammasome signaling. Cell *163*, 1428–1443.

Li, P., Allen, H., Banerjee, S., Franklin, S., Herzog, L., Johnston, C., McDowell, J., Paskind, M., Rodman, L., Salfeld, J., et al. (1995). Mice deficient in IL-1 beta-converting enzyme are defective in production of mature IL-1 beta and resistant to endotoxic shock. Cell *80*, 401–411.

Man, S.M., Tourlomousis, P., Hopkins, L., Monie, T.P., Fitzgerald, K.A., and Bryant, C.E. (2013). *Salmonella* infection induces recruitment of Caspase-8 to the inflammasome to modulate IL-1β production. J. Immunol. *191*, 5239–5246.

Mariathasan, S., Newton, K., Monack, D.M., Vucic, D., French, D.M., Lee, W.P., Roose-Girma, M., Erickson, S., and Dixit, V.M. (2004). Differential activation of the inflammasome by caspase-1 adaptors ASC and Ipaf. Nature *430*, 213–218.

Masumoto, J., Dowds, T.A., Schaner, P., Chen, F.F., Ogura, Y., Li, M., Zhu, L., Katsuyama, T., Sagara, J., Taniguchi, S., et al. (2003). ASC is an activating adaptor for NF-kappa B and caspase-8-dependent apoptosis. Biochem. Biophys. Res. Commun. *303*, 69–73.

Miao, E.A., Leaf, I.A., Treuting, P.M., Mao, D.P., Dors, M., Sarkar, A., Warren, S.E., Wewers, M.D., and Aderem, A. (2010). Caspase-1-induced pyroptosis is an innate immune effector mechanism against intracellular bacteria. Nat. Immunol. *11*, 1136–1142.

Miyoshi, H., and Stappenbeck, T.S. (2013). In vitro expansion and genetic modification of gastrointestinal stem cells in spheroid culture. Nat. Protoc. *8*, 2471–2482.

Müller, A.A., Dolowschiak, T., Sellin, M.E., Felmy, B., Verbree, C., Gadient, S., Westermann, A.J., Vogel, J., LeibundGut-Landmann, S., and Hardt, W.D. (2016). An NK cell perforin response elicited via IL-18 controls mucosal inflammation kinetics during *Salmonella* gut infection. PLoS Pathog. *12*, e1005723.

Nordlander, S., Pott, J., and Maloy, K.J. (2014). NLRC4 expression in intestinal epithelial cells mediates protection against an enteric pathogen. Mucosal Immunol. *7*, 775–785.

Rauch, I., Tenthorey, J.L., Nichols, R.D., Al Moussawi, K., Kang, J.J., Kang, C., Kazmierczak, B.I., and Vance, R.E. (2016). NAIP proteins are required for cytosolic detection of specific bacterial ligands in vivo. J. Exp. Med. *213*, 657–665.

Romberg, N., Al Moussawi, K., Nelson-Williams, C., Stiegler, A.L., Loring, E., Choi, M., Overton, J., Meffre, E., Khokha, M.K., Huttner, A.J., et al. (2014). Mutation of NLRC4 causes a syndrome of enterocolitis and autoinflammation. Nat. Genet. *46*, 1135–1139.

Rosenblatt, J., Raff, M.C., and Cramer, L.P. (2001). An epithelial cell destined for apoptosis signals its neighbors to extrude it by an actin- and myosin-dependent mechanism. Curr. Biol. *11*, 1847–1857.

Sasaki, Y., Derudder, E., Hobeika, E., Pelanda, R., Reth, M., Rajewsky, K., and Schmidt-Supprian, M. (2006). Canonical NF-kappaB activity, dispensable for B cell development, replaces BAFF-receptor signals and promotes B cell proliferation upon activation. Immunity *24*, 729–739.

Sato, T., and Clevers, H. (2013). Primary mouse small intestinal epithelial cell cultures. Methods Mol. Biol. *945*, 319–328.

Sellin, M.E., Müller, A.A., Felmy, B., Dolowschiak, T., Diard, M., Tardivel, A., Maslowski, K.M., and Hardt, W.-D. (2014). Epithelium-intrinsic NAIP/NLRC4 inflammasome drives infected enterocyte expulsion to restrict *Salmonella* replication in the intestinal mucosa. Cell Host Microbe *16*, 237–248.

Sellin, M.E., Maslowski, K.M., Maloy, K.J., and Hardt, W.-D. (2015). Inflammasomes of the intestinal epithelium. Trends Immunol. *36*, 442–450.

Shi, J., Zhao, Y., Wang, K., Shi, X., Wang, Y., Huang, H., Zhuang, Y., Cai, T., Wang, F., and Shao, F. (2015). Cleavage of GSDMD by inflammatory caspases determines pyroptotic cell death. Nature *526*, 660–665.

Srinivas, S., Watanabe, T., Lin, C.S., William, C.M., Tanabe, Y., Jessell, T.M., and Costantini, F. (2001). Cre reporter strains produced by targeted insertion of EYFP and ECFP into the ROSA26 locus. BMC Dev. Biol. *1*, 4.

Strowig, T., Henao-Mejia, J., Elinav, E., and Flavell, R. (2012). Inflammasomes in health and disease. Nature *481*, 278–286.

von Moltke, J., Trinidad, N.J., Moayeri, M., Kintzer, A.F., Wang, S.B., van Rooijen, N., Brown, C.R., Krantz, B.A., Leppla, S.H., Gronert, K., and Vance, R.E. (2012). Rapid induction of inflammatory lipid mediators by the inflammasome in vivo. Nature *490*, 107–111.

Wang, H., Yang, H., Shivalila, C.S., Dawlaty, M.M., Cheng, A.W., Zhang, F., and Jaenisch, R. (2013). One-step generation of mice carrying mutations in multiple genes by CRISPR/Cas-mediated genome engineering. Cell *153*, 910–918.

Wlodarska, M., Thaiss, C.A., Nowarski, R., Henao-Mejia, J., Zhang, J.-P., Brown, E.M., Frankel, G., Levy, M., Katz, M.N., Philbrick, W.M., et al. (2014). NLRP6 inflammasome orchestrates the colonic host-microbial interface by regulating goblet cell mucus secretion. Cell *156*, 1045–1059.

Zhang, L., Chen, S., Ruan, J., Wu, J., Tong, A.B., Yin, Q., Li, Y., David, L., Lu, A., Wang, W.L., et al. (2015). Cryo-EM structure of the activated NAIP2-NLRC4 inflammasome reveals nucleated polymerization. Science *350*, 404–409.

Zhao, Y., Yang, J., Shi, J., Gong, Y.-N., Lu, Q., Xu, H., Liu, L., and Shao, F. (2011). The NLRC4 inflammasome receptors for bacterial flagellin and type III secretion apparatus. Nature *477*, 596–600.